Modelling the leaching of Pb, Cd, As, and Cr from cementitious waste using PHREEQC

Cheryl E. Halim [a], Stephen A. Short [b], Jason A. Scott [a], Rose Amal [a,*], Gary Low [c]

[a] *ARC Centre for Functional Nanomaterials, School of Chemical Engineering and Industrial Chemistry, The University of New South Wales, Sydney, NSW 2052, Australia*
[b] *Ecoengineers Pty. Ltd., 9 Sunninghill Circuit, Mount Ousley, NSW 2519, Australia*
[c] *Department of Environment and Conservation, Analytical and Environmental Chemistry Section, Lidcombe, NSW 2141, Australia*

Abstract

A leaching model was developed using the United States Geological Survey public domain PHREEQC geochemical package to simulate the leaching of Pb, Cd, As, and Cr from cementitious wastes. The model utilises both kinetic terms and equilibrium thermodynamics of key compounds and provides information on leachate and precipitate speciation. The model was able to predict the leaching of Pb, Cd, As, and Cr from cement in the presence of both simple (0.1 and 0.6 M acetic acid) and complex municipal landfill leachates. Heavy metal complexation by the municipal landfill leachate was accounted for by the introduction of a monoprotic organic species into the model.

The model indicated Pb and As were predominantly incorporated within the calcium silicate hydrate matrix while a greater portion of Cd was seen to exist as discrete particles in the cement pores and Cr (VI) existed mostly as free CrO_4^{2-} ions. Precipitation was found to be the dominant mechanism controlling heavy metal solubility with carbonate and silicate species governing the solubility of Pb and carbonate, silicate and hydroxide species governing the solubility of Cd. In the presence of acetic acid, at low pH values Pb and Cd acetate complexes were predominant whereas, at high pH values, hydroxide species dominated. At high pH values, the concentration of As in the leachate was governed by the solubility of $Ca_3(AsO_4)_2$ with the presence of carbonate alkalinity competing with arsenate for Ca ions. In the presence of municipal landfill leachate, Pb and Cd organic complexes dominated the heavy metal species in solution. The reduction of As and Cr in municipal landfill leachate was crucial for determining aqueous speciation, with typical municipal landfill conditions providing the reduced forms of As and Cr.
Published by Elsevier B.V.

Keywords: Cementitious waste; PHREEQC; Geochemical modelling; Lead; Cadmium; Arsenic; Chromium; Municipal landfill; Leachate

1. Introduction

In recent years there have been increased concerns regarding the leaching of hazardous substances from landfills into local surroundings. As a result, an extensive array of leaching tests has been developed to assess the hazards of heavy metal-containing wastes prior to disposal. Failure to pass a regulatory leaching test typically necessitates some form of waste stabilisation, such as cement addition. Batch leaching tests are the preferred choice for regulatory assessment due to their simplicity, improved reproducibility, and shorter time requirements. However, as batch leaching tests are typically run over short time frames, it is debatable whether the compounds of interest behave similarly in the long term. Modelling can potentially predict the long term leaching of wastes providing a solution to problems inherent to batch procedures. A model capable of describing contaminant leaching from wastes can assist in improving the development of management options [1].

This study focuses on the leaching of Pb, Cd, As, and Cr from cement-stabilised waste. The leaching of heavy metal ions from cementitious waste has been extensively investi-

* Corresponding author. Tel.: +61 2 93854361; fax: +61 2 93855966.
E-mail address: r.amal@unsw.edu.au (R. Amal).

gated [2–7], with many researchers using physical mechanistic leaching models [8–11]. Although physical mechanistic models can successfully describe the leaching of contaminants from cement, this approach does not give direct indication of chemical species controlling the release. According to van der Sloot et al. [1], the chemistry of elements and their interaction with substances present in the leaching fluid, including ligands and sorbing phases, are governing factors in element release. Geochemical modelling enables quantitative speciation of elements based on species stability constants. PHREEQC is a geochemical modelling package capable of describing chemical reactions and transport processes in water. It is based on the equilibrium chemistry of aqueous solutions with other components, such as minerals, gases, solid solutions, and sorbing surfaces. A solid solution forms when compounds containing similar properties, such as size and charge, precipitate to form a homogeneous solid compound. It is also capable of incorporating kinetic equations for chemical reactions and determining speciation at any designated time. Many models have been developed to describe the chemistry of natural waters [12] but at present no model of this type has been developed to describe the leaching of elemental contaminants from cement.

This paper presents work aimed at using PHREEQC to develop a model for simulating the leaching of Pb, Cd, As, and Cr from cementitious wastes and, where possible, identify species governing the release of these contaminants. Model outcomes were assessed by comparison with leaching profiles obtained from procedures recommended by AS 4439.3-1997. Leaching fluids studied included 0.1 and 0.6 M acetic acid and a municipal landfill (ML) leachate.

2. Experimental procedure

2.1. Preparation of cementitious waste

Cementitious wastes were prepared by mixing Type GP Ordinary Portland Cement (OPC), supplied by Australian Cement (in accordance with Australian Standard AS 3972-1991), with solutions of lead nitrate ($Pb(NO_3)_2$), cadmium nitrate tetrahydrate ($Cd(NO_3)_2 \cdot 4H_2O$), sodium arsenate ($Na_2HAsO_4 \cdot 7H_2O$), or sodium chromate (Na_2CrO_4) such that they contained 2.34% Pb, 1.3% Cd, 1.3% As, or 2.0% Cr by weight, respectively. The metal salts were dissolved in water, mechanically blended with the OPC and cured for 28 days at water to cement ratios of 0.38 (Pb-spiked cement), 0.44 (Cd-spiked cement), 0.38 (As-spiked cement), and 0.31 (Cr-spiked cement). Detailed procedures are further described in a previous publication [13]. The cured mixtures were crushed by three consecutive crushers (jaw crusher, cone crusher, and roller crusher), and passed through a 2.4-mm mesh sieve. The compositions of the cement samples were analysed using X-ray fluorescence (XRF) and are shown in Table 1.

Table 1
Composition of cementitious wastes (dry weight) containing Pb, Cd, As, and Cr as determined by X-ray fluorescence [49]

Element	Cement composition (mg g^{-1} of waste)			
	Pb cement	Cd cement	As cement	Cr cement
Pb	23	0.0	0.0	0.0
Cd	0.0	13	0.0	0.0
As	0.0	0.0	13	0.0
Cr	0.0	0.0	0.0	20
Al	16	15	16	15
C	15	20	11	9
Ca	340	340	340	340
Fe	23	22	23	23
K	6.6	7.5	6.6	6.6
Mg	10	10	10	10
Na	4.5	2.2	13	22
Si	74	73	74	73
S	8.8	8.4	8.8	8.8
Th	0.9	0.9	0.9	0.9
Ti	0.6	0.6	0.6	0.6

2.2. Leaching experiments

The leaching procedure used was that recommended by Australian Standard AS 4439.3-1997 [14]. AS 4439.3-1997 is a modified version of the toxicity characteristic leaching procedure (TCLP), designed to account for waste disposal scenarios other than and including codisposal in a municipal solid waste landfill [14]. Eighty grams of crushed waste was tumbled with 1600 g of leaching fluid at a speed of 30 rpm. Approximately ten 10-mL samples were taken at nominated time intervals between 0 and 7 days. The zero-hour value corresponds to sample mixed with the leaching fluid for a few seconds prior to tumbling. Leachate samples were filtered by a 0.8-micron membrane filter and analysed for metal ions using an Optima 3000 Inductively Coupled Plasma Atomic Emission Spectroscope (ICP AES).

Leaching fluids used included 0.1 and 0.6 M acetic acid solutions and a municipal landfill leachate. 0.1 M acetic acid is a leaching fluid recommended by AS 4439.3-1997 whereas 0.6 M acetic acid was utilised for comparison with ML leachate on the basis of final pH. That is, both leachants attained a final pH of between 10 and 12 after 7 days leaching. The ML leachate was collected in seven 20-L drums (no headspace) from a pipe leading to a leachate pond in a mature landfill (~20 years old). The landfill received both putrescible and non-putrescible wastes. Approximately 4 L of sample was taken from each drum for characteristic analyses, with the remainder stored at 4 °C. Leachate samples utilising acetic acid as the leaching fluid were preserved by 2% (v/v) HNO_3 addition while the ML leachate samples were stored at 4 °C to minimise microbial activity. Composition of the ML leachate is provided in Table 2. Detailed descriptions of landfill properties, leachate collection, and analytical procedures are described elsewhere [13].

Table 2
Composition of the municipal landfill leachate

Leachate characteristics	Municipal landfill leachate
pH	7.8 ± 0.1
BOD$_5$	840 ± 230
COD	3850 ± 130
Conductivity ($\mu S\,cm^{-1}$)	24000 ± 3500
Dissolved inorganic carbon	1900 ± 700
Dissolved organic carbon	500 ± 300
Aluminium	0.9 ± 0
Ammonium[a]	2800 ± 100
Calcium	92 ± 25
Chloride	2900 ± 410
Iron	14 ± 1
Magnesium	120 ± 5
Phosphate	16 ± 4
Potassium	1400 ± 300
Sodium	1700 ± 300
Sulfate	32 ± 33

All values are in $mg\,L^{-1}$ except for pH and where indicated.

[a] Calculated from NH$_3$–N level.

3. Establishment of PHREEQC simulation for metal leaching from cement

PHREEQC Version 2 was used to model the leaching of contaminants from cementitious wastes. Thermodynamic data was obtained from the Lawrence Livermore National Library (LLNL) database. The database was modified to include thermodynamic data for highly alkaline, and high Ca and Si systems (provided by Atkins et al. [15] and Berner [16]), and the US EPA MINTEQ database [17]. The thermodynamic data of CaH_2SiO_4 (C–S–H gel) employed was consistent with the Berner model for OPC [18].

3.1. Model input

Hydrated Portland cement primarily contains hydrated calcium silicates (40–50%, w/w) and portlandite ($Ca(OH)_2$) (20–25%, w/w). The remainder comprises of tricalcium aluminate and calcium aluminoferrite (10–20%, w/w), pore solution (10–20%, w/w), and soluble components (alkalihydroxides) (0–5%, w/w) [16]. In the model simulation, cement was classified into four distinct groups: C–S–H matrix; portlandite; calcite (portlandite that had adsorbed atmospheric CO_2); and free heavy metal compounds. The portlandite and calcite matrices were assumed to contain only $Ca(OH)_2$ and $CaCO_3$, respectively. The C–S–H matrix was assumed to contain C–S–H gel, hydrogarnet ($Ca_3Al_2(H_4O_4)_3$), brownmillerite ($Ca_4Al_2Fe_2O_{10}$), NaOH, KOH, $Mg(OH)_2$, $CaSO_4$, and a portion of the heavy metal compounds studied ($Pb(OH)_2$, $Cd(OH)_2$, $Ca_3(AsO_4)_2$, or CrO_4^{2-}). C–S–H gel, hydrogarnet, and brownmillerite were chosen to represent the solubility-controlling phases, according to the findings by Geelhoed et al. [19] for cement-like chromite ore processing residue. The remaining heavy metal ions ($Pb(OH)_2$, $Cd(OH)_2$, CrO_4^{2-}, or $Ca_3(AsO_4)_2$) were considered available to form free compounds not associated with the C–S–H

matrix within the cement pores. Values were assumed to be 18% for Pb, 56% for Cd, 12% for As, and 68% for Cr with respect to the total Pb, Cd, As, and Cr contents in cement and were estimated by fitting experimental time-dependant leach data to earlier Electron Microprobe findings. They showed Pb and As to be predominantly dispersed throughout the C–S–H matrix and Cd to be mainly present as discrete particles [20]. However, 44% of the Cd was assumed to be dispersed in the C–S–H matrix to model Cd trapped within the C–S–H pores. Arsenic was assumed to be present as calcium arsenate, as described by Mollah et al. [21] and believed to exist in the hydration products. This assumption derived from difficulties in identifying the actual form of arsenic in cement and the lack of available thermodynamic data describing the dissolution of complex arsenic compounds. Chromium was specified to exist as free chromate ions, which were mostly soluble and not incorporated in the C–S–H matrix. Previous experiments indicated chromium possessed a high solubility, suggesting Cr may only be adsorbed on the surface of cement or form soluble chromium compounds [20]. This is consistent with Geelhoed et al. [19], who proposed the formation of Cr(VI)-bearing hydrogarnet, Cr(VI)-hydrocalumite, and Cr(VI)-ettringite in cement, all of which have a high solubility.

The absolute metal compositions in each matrix were calculated based on the actual amounts of the elements as determined by XRF (Table 1). This assumes no residual unhydrated CaO, SiO_2, Al_2O_3, and Fe_2O_3 was present. The amount of C–S–H gel was based on the Si content (Table 1), the amount of calcite on the C content, the amount of gypsum on the S content, and the amount of brownmillerite on the Fe content. The amount of hydrogarnet was calculated by subtraction of the Al content of the brownmillerite from the total Al content. The portlandite content was calculated by subtraction of the amounts of Ca in the C–S–H gel, calcite, gypsum, hydrogarnet, and brownmillerite from the total Ca content.

During data entry, the amount of each matrix accessible to the leaching fluids requires specification. Input values are shown in Table 3. Also indicated are the portions of cement matrix available for acid attack. It was assumed 100% of the matrix was available for acid attack in the presence of 0.6 M acetic acid, while 31 and 25% was available for acid attack when 0.1 M acetic acid and municipal landfill leachate were used, respectively. These are bulk scaling factors, representing the overall efficiency of solid/liquid mass transfer out of the cement matrix, with a higher acid concentration providing a higher mass transfer of metal ions. These values were obtained by trial and error, based on experimental leaching data. Hinsenveld [11] suggested that increasing leachant acidity may also increase the release of metals adsorbed on the cement surface and allow access to compounds not normally leached at low acid strengths. Such possibilities were used to avoid greater model complexity through attempting to account for diffusive and surface area controls. However, the maximum theoretical amount of calcite was specified for

Table 3
Available amounts of cement components for acid attack by different leaching fluids

Matrices	Available concentrations of cement components (mg 50g^{-1} of waste)											
	0.1 M acetic acid				0.6 M acetic acid				Municipal landfill leachate			
	Pb cement	Cd cement	As cement	Cr cement	Pb cement	Cd cement	As cement	Cr cement	Pb cement	Cd cement	As cement	Cr cement
Bulk mass transfer factor	31%	31%	31%	31%	100%	100%	100%	100%	25%	25%	25%	25%
Portlandite	5.2×10^{-2}	4.3×10^{-2}	5.3×10^{-2}	6.0×10^{-2}	1.7×10^{-1}	1.4×10^{-1}	1.7×10^{-1}	1.9×10^{-1}	4.3×10^{-2}	3.5×10^{-2}	4.4×10^{-2}	4.8×10^{-2}
Calcite	6.3×10^{-2}	8.3×10^{-2}	4.6×10^{-2}	3.8×10^{-2}	6.3×10^{-2}	8.3×10^{-2}	4.6×10^{-2}	3.8×10^{-2}	6.3×10^{-2}	8.3×10^{-2}	4.6×10^{-2}	3.8×10^{-2}
C–S–H matrix	6.1×10^{-2}	6.1×10^{-2}	6.9×10^{-2}	7.5×10^{-2}	2.0×10^{-1}	2.0×10^{-1}	2.2×10^{-1}	2.4×10^{-1}	5.3×10^{-2}	4.9×10^{-2}	5.5×10^{-2}	6.0×10^{-2}
Free Pb(OH)$_2$	3.1×10^{-4}	–	–	–	1.0×10^{-3}	–	–	–	2.5×10^{-4}	–	–	–
Free Cd(OH)$_2$	–	1.0×10^{-3}	–	–	–	3.3×10^{-3}	–	–	–	8.3×10^{-4}	–	–
Free Ca$_3$(AsO$_4$)$_2$	–	–	1.6×10^{-4}	–	–	–	5.0×10^{-4}	–	–	–	1.3×10^{-4}	–
Free CrO$_4{}^{2-}$	–	–	–	6.0×10^{-3}	–	–	–	1.3×10^{-2}	–	–	–	6.0×10^{-3}

each leaching fluid as it was assumed to be entirely contained on the cement surface and therefore readily available for leaching. Initially, a higher level of free chromate ions was specified, relative to that present in the bulk matrix, as it was assumed the easily soluble chromate is more readily available than chromate in the portlandite and C–S–H matrix. This is in accordance with previous findings [8], which showed a greater percentage of Cr release compared to Ca release, indicating the highly soluble nature of Cr. Mole percents of the compounds specified in the C–S–H matrix and their thermodynamic data are shown in Table 4, indicating the proportional amounts estimated to be available for leaching from the C–S–H matrix.

A schematic of the developed modelling algorithms is shown in Fig. 1. The model commences with the kinetics of cement dissolution, illustrating the release of cement components as the waste is mixed with the leaching fluid. Leaching fluids were defined to be either 0.1 M acetic acid (pH 2.88), 0.6 M acetic acid (pH 2.5), or municipal landfill leachate (pH 7.0) (Table 5). Oxidising conditions were maintained for the acetic acid solutions (pe 4.0—default pe in PHREEQC). The municipal landfill leachate was assigned an initial reducing condition of pe −3.1 (corresponding to −183 mV at 25 °C), to lie within the range of typical landfill leachate redox potentials (−100 to −300 mV) [22]. For the acetic acid leachants, acetate was defined in the input file at concentrations of either 0.1 or 0.6 M. Input definitions for the municipal landfill leachate included 0.0092 M of Organic X and 0.16 M of carbonate ions (based on dissolved organic and inorganic carbon in the leachate), with other major cation and anion contents determined from the values given in Table 2. The Organic X content was estimated based on 500 mg L^{-1} of dissolved organic carbon in the leachate (Table 2) coupled with the assumption that 45% of the carbon existed as dissolved organic matter having a molecular weight of 121. This composition is typical for landfill leachates as determined by Brown et al. [23]. Initial leachate compositions and corresponding thermodynamic data are shown in Table 5.

The quantities of metal ions released from the cement over any defined leaching period are determined by the cement dissolution kinetics. At each specified time step, PHREEQC resolves metal speciation in both the solid and solution forms by establishment of a thermodynamic equilibrium. This occurs through complexation with organic ligands, formation of solid solutions, solid/liquid equilibrium, and adsorption onto hydrous ferric oxides and silica gel. Greater detail on each module is provided in the following sections.

3.2. Dissolution rates

According to Berner [24], concrete dissolution can be described by several stages. Cement degradation begins with the dissolution of alkali hydroxides and free portlandite, followed by dissolution of calcium silicates, calcium aluminates, calcium aluminosulfates, and Mg(OH)$_2$, with unhydrated SiO$_2$, Al$_2$O$_3$, and Fe$_2$O$_3$ being last to dissolve. The

Table 4
Mole percents of metal compounds in the C–S–H matrix

Compounds	Mol% in the matrix				log solubility constant (K_{sp}) or neutralisation constant[a] (K_n)
	Pb cement	Cd cement	As cement	Cr cement	
C–S–H gel (CaH_2SiO_4)	64.5	66.6	59.5	54.4	$K_n = 15.30$[b]
Hydrogarnet ($Ca_3Al_2(H_4O_4)_3$)	2.2	2.2	2.2	1.4	$K_n = 81.45$[c]
Brownmillerite ($Ca_4Al_2Fe_2O_{10}$)	5.1	5.1	4.7	4.3	$K_n = 140.51$[d]
Gypsum ($CaSO_4 \cdot 2H_2O$)	6.7	6.7	6.2	5.7	$K_{sp} = -4.31$[d]
KOH[e]	4.2	4.9	3.8	3.5	N/A[f]
$Mg(OH)_2$	10.3	10.7	9.5	8.8	$K_n = 16.30$[d]
NaOH[e]	4.7	2.5	12.4	19.4	N/A[f]
$Pb(OH)_2$ in C–S–H	2.3	–	–	–	$K_n = 12.64$[g,d]
$Cd(OH)_2$ in C–S–H	–	1.3	–	–	$K_n = 13.74$[d]
$Ca_3(AsO_4)_2$ in C–S–H	–	–	1.7	–	$K_n = 17.82$[d]
CrO_4^{2-}[e] in C–S–H	–	–	–	2.5	N/A[f]

[a] Neutralisation constant (based on reaction of the metal compound with H^+).
[b] Taken from [18].
[c] Taken from [50].
[d] Taken from [51].
[e] NaOH, KOH and CrO_4^{2-} assumed present as soluble species.
[f] Not applicable.
[g] Neutralisation constant of litharge ($PbO + 2H^+ = H_2O + Pb^{2+}$).

cement sample in this study contained a significant amount of calcite as shown by the level of carbon in the sample (Table 1). This may be due to carbonation during sampling, leaving only a small amount of portlandite on the surface. The dissolution rates of the four matrices in cement are described in Eq. (1), with the constants for each matrix tabulated in Table 6. The basic form of Eq. (1) was obtained from the calcite dissolution rate described by Chou et al. [25].

$$\frac{dM}{dt} = 50 \times 10^4 k_{system} A(c_1 a_{H^+} + c_2 a_{H_2CO_3} + c_3 a_{OH^-} - c_4 a_{Ca^{2+}} a_{CO_3^{2-}} + c_5) \tag{1}$$

where dM/dt is the dissolution rate of each matrix (calcite, portlandite, C–S–H matrix, and the free metal compounds); k_{system} is a constant; A is the surface area of the matrix (in $m^2 g^{-1}$ of waste); and $a_{H^+}, a_{H_2CO_3}, a_{OH^-}, a_{Ca^{2+}},$ and $a_{CO_3^{2-}}$ are the activities of $H^+, H_2CO_3, OH^-, Ca^{2+},$ and CO_3^{2-}, respectively. Values in brackets are in $mol\, cm^{-2}\, s^{-1}$. The dissolution rate was converted to 50 g of waste/L of solution by the factor "50" while the "10^4" factor converts surface area units from $m^2 g^{-1}$ to $cm^2 g^{-1}$.

BET N_2 adsorption measurements found the surface area of the cement sample varied between 65 and 87 $m^2 g^{-1}$. It was assumed C–S–H gel dominated the surface area as C–S–H gel consists of much smaller particles than portlandite and calcite, as seen in SEM images from Kjellsen and Justnes [26]. Therefore, a surface area of 70 $m^2 g^{-1}$ of sample was attributed to the C–S–H component. The portlandite particle size was approximated by a cylinder of diameter 4 μm and length 10 μm [27]. The calcite particles were assumed to be cubic in shape with a width of 10 μm [28]. These
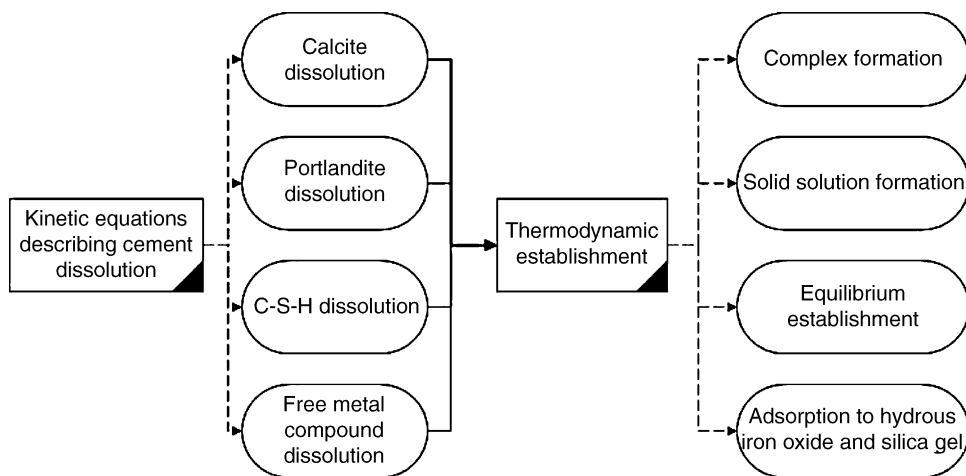

Fig. 1. Schematic diagram of the modelling algorithms.

Table 5
Initial concentration of leachate components upon exposure of metal contaminated cements to acetic acid or municipal landfill leachate

Compounds	Initial concentration (mol L^{-1})				log formation constant (K_f) or neutralisation constant (K_n)[a] or dissociation constant (K_d)
	Pb-contaminated cement	Cd-contaminated cement	As-contaminated cement	Cr-contaminated cement	
Acetate[b]	0.1/0.6	0.1/0.6	0.1/0.6	0.1/0.6	$K_d = -4.76$[c,d]
CO_3[e]	0.16	0.16	0.16	0.16	$K_d = -10.33$[c,f]
Organic X[e]	0.0092	0.0092	0.0092	0.0092	–
Na[e]	0.074	0.074	0.074	0.074	–
K[e]	0.036	0.036	0.036	0.036	–
Mg[e]	0.0050	0.0050	0.0050	0.0050	–
Cl[e]	0.082	0.082	0.082	0.082	–
NH_4[e]	0.16	0.16	0.16	0.16	–
P[e]	0.00052	0.00052	0.00052	0.00052	–
S[e]	0.00048	0.00048	0.00048	0.00048	–
Complex species					
PbOrganic X$^+$	0	–	–	–	$K_f = 9.40$[g]
PbOrganic X$_2$	0	–	–	–	$K_f = 10.40$[g]
PbOrganic X$_3{}^-$	0	–	–	–	$K_f = 11.40$[g]
CdOrganic X$^+$	–	0	–	–	$K_f = 7.60$[g]
CdOrganic X$_2$	–	0	–	–	$K_f = 8.40$[g]
CdOrganic X$_3{}^-$	–	0	–	–	$K_f = 9.90$[g]
Adsorbed species[h]					
Hfo_sOPb$^+$	0	–	–	–	$K_d = 4.65$[c,i]
Hfo_wOPb$^+$	0	–	–	–	$K_d = 0.30$[c,i]
Surf_sOPb$^+$	0	–	–	–	$K_d = -7.75$[i,j]
(Surf_sO)$_2$Pb	–	0	–	–	$K_d = -17.23$[i,j]
Hfo_sOCd$^+$	–	0	–	–	$K_d = 0.47$[c,i]
Hfo_wOCd$^+$	–	0	–	–	$K_d = -2.91$[c,i]
Surf_sOCd$^+$	–	0	–	–	$K_d = -10.40$[i,j]
Hfo_wH$_2$AsO$_4$	–	–	0	–	$K_f = 29.31$[i]
Hfo_wHAsO$_4{}^-$	–	–	0	–	$K_f = 23.51$[i]
Hfo_wOHAsO$_4{}^{3-}$	–	–	0	–	$K_f = 10.58$[i]
Hfo_wCrO$_4{}^-$	–	–	–	0	$K_f = 10.29$[i]
Hfo_sCrO$_4{}^-$	–	–	–	0	$K_f = 10.29$[i]
Solid solution					
Fe(OH)$_3$	0	0	0	0	$K_n = 5.66$[c]
Gibbsite (Al(OH)$_3$)	0	0	0	0	$K_n = 7.76$[c]
Litharge (PbO)	0	0	0	0	$K_n = 12.64$[c,k]
Ca$_3$(AsO$_4$)$_2$	0	0	0	0	$K_n = 17.82$[c]

[a] Neutralisation constant (based on reaction of the metal compound with H$^+$).

[b] 0.1 or 0.6 M acetic acid used as leaching fluid.

[c] Taken from [51].

[d] Dissociation constant (HAcetate = H$^+$ + acetate$^-$).

[e] Municipal landfill leachate used as leaching fluid.

[f] Constant for dissociation of HCO$_3{}^-$ to CO$_3{}^{2-}$ (HCO$_3{}^-$ = CO$_3{}^{2-}$ + H$^+$).

[g] Organic complexation formation constant/conditional stability constant (M^{n+} + y Organic X$^-$ = MOrganic X$_y{}^{n-y}$ where M is a metal ion, Organic X is an organic ligand, and n and y are constants). Values chosen as they provide a good fit for Pb and Cd leachate concentrations.

[h] Hfo represents hydrous ferric oxide surface: Hfo_w represents weak surface adsorption; Hfo_s represents strong surface adsorption. Surf_s represents surface silanol groups.

[i] Constant describing surface complex formation (SurfaceOH + M^{n+} = SurfaceOM$^{(n-1)+}$ + H$^+$ where M is metal ion).

[j] Taken from [42].

[k] Neutralisation constant of litharge (PbO + 2H$^+$ = H$_2$O + Pb^{2+}).

definitions correspond to surface areas of 490 μm^2/calcite particle and 150 μm^2/portlandite particle and weights of 2.0×10^{-9} g/calcite particle and 2.8×10^{-9} g/portlandite particle. Calcite and portlandite densities were obtained from Joye and Demont [29]. Portlandite and calcite surface areas per gram of sample were estimated from the mass compositions and particle sizes. Significantly smaller surface areas were selected for free Pb(OH)$_2$, Cd(OH)$_2$, Ca$_3$(AsO$_4$)$_2$, and CrO$_4{}^{2-}$ due to their low relative contents in the cement. Constant surface area with time was assumed in this simulation.

The rate constants for calcite dissolution (c_1, c_2, c_4, c_5) were based on values obtained by Chou et al. [25]. To account for the different mixing process in this study (tumbling) compared to Chou et al. (continuous fluidised bed reactor), and the therefore different diffusion processes, a constant "k_{system}" was introduced. The portlandite dissolution rate

Table 6
Dissolution rate constants of cement as described in Eq. (1)

M	k_{system}	A (m² g⁻¹)				Rate constants (mol cm⁻² s⁻¹ M⁻¹)				
		Pb cement	Cd cement	As cement	Cr cement	c_1	c_2	c_3	c_4	c_5
Calcite	0.77	0.04	0.05	0.02	0.02	$10^{-4.05a}$	$10^{-7.30a}$	–	$10^{-1.72a}$	$10^{-10.2a}$
Portlandite	0.77	0.13	0.13	0.14	0.15	$10^{-2.95b}$	–	–	–	$10^{-9.19b}$
C–S–H matrix	0.77	70	70	70	70	$10^{-7.88b}$	–	$10^{-9.53b}$	–	–
Free Pb(OH)₂	0.77	0.01	–	–	–	$10^{-2.95b}$	–	–	–	$10^{-9.19b}$
Free Cd(OH)₂	0.77	–	0.01	–	–	$10^{-2.95b}$	–	–	–	$10^{-9.19b}$
Free Ca₃(AsO₄)₂	0.77	–	–	0.01	–	$10^{-2.95b}$	–	–	–	$10^{-9.19b}$
Free CrO₄²⁻	0.77	–	–	–	0.01	$10^{-2.8b}$	–	$10^{-3.50b}$	–	–

[a] Taken from [25].
[b] Fitted to experimental data.

was described in a similar manner to calcite dissolution. Portlandite dissolution was defined as only being governed by the presence of H^+. Higher rate constants to depict the faster dissolution rate of portlandite over calcite [30] were also used. These constants generate slightly higher portlandite dissolution rates ($10^{-7.9}$ and $10^{-9.1}$ mol cm⁻² s⁻¹ at pH 5 and 7, respectively) compared to CaO ($10^{-8.4}$ and $10^{-9.5}$ mol cm⁻² s⁻¹ at pH 5 and 7, respectively), as indicated by Segall et al. [31]. The difference in values is reasonable as oxide dissolution should be slower than hydroxide dissolution due the oxide requiring a hydration step prior to dissociation of the hydroxide.

Dissolution rate constants of the C–S–H matrix, which were unable to be located in the literature, were set at much lower values than calcite and portlandite as it is widely recognised that C–S–H disintegration occurs at slower rate than these two minerals [24]. While it is well known that C–S–H dissolution is strongly influenced by H^+ [32], other studies have suggested OH^- may also play a role [33]. Dissolution also releases other compounds present in the C–S–H matrix (Table 3) in amounts proportional to their relative compositions (Table 4). Free metal compound (Pb(OH)₂, Cd(OH)₂, and Ca₃(AsO₄)₂) dissolution was defined to have the same rate constants as portlandite dissolution, and only to be influenced by the H^+ term as the metal hydroxides were assumed to have the same accessibility to the leachate as portlandite. The rate of dissolution of free CrO_4^{2-} dispersed through the C–S–H gel phase was assumed to be influenced by both H^+ and OH^-. The assigned rate constants were higher than both portlandite and C–S–H dissolution as it was previously observed that a higher degree of leaching was obtained for Cr than Ca in the cement system [20].

The same cement dissolution rate constants were used for all leaching fluids. Variations are only associated with leaching fluid compositions and the maximum availability of cement components (portlandite, C–S–H matrix, and free metal ion) to dissolve (Table 3).
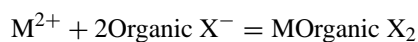
3.3. Complex formation

The complicated nature of ML leachate makes it extremely difficult to identify organic materials in the leachate available to complex with the metal cations. Therefore, a monoprotic Organic X was selected. Complexation reactions of Organic X with Pb and Cd, cations, (represented by (M^{2+})) are shown in Eqs. (2)–(4). As As and Cr were added as anions, their complexation was assumed negligible.

$$M^{2+} + \text{Organic X}^- = \text{MOrganic X}^+$$
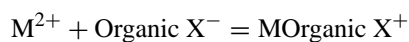
$$K_1 = \frac{[\text{MOrganic X}^+]}{([M^{2+}][\text{Organic X}^-])} \qquad (2)$$

$$M^{2+} + 2\text{Organic X}^- = \text{MOrganic X}_2$$

$$K_2 = \frac{[\text{MOrganic X}_2]}{([M^{2+}][\text{Organic X}^-]^2)} \qquad (3)$$

$$M^{2+} + 3\text{Organic X}^- = \text{MOrganic X}_3^-$$
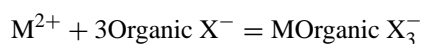
$$K_3 = \frac{[\text{MOrganic X}_3^-]}{([M^{2+}][\text{Organic X}^-]^3)} \qquad (4)$$

The log values of K_1, K_2, and K_3 are provided in Table 5. These were estimated such that Pb and Cd release profiles agreed with experimental results. Although typical conditional stability constants of Pb and Cd complexes in landfill leachates are not readily available, the values used here are comparable to those measured by Muller [34] for Pb and Cd complexation with dissolved, colloidal, and particulate matter in estuarine and coastal waters (log K between 9.5–12.5 for Pb and 9.5–10.5 for Cd). The lower stability constants for Cd, compared to Pb, are also consistent with other studies [34,35].

3.4. Solid solution formation, adsorption on hydrous iron oxides, and equilibrium state of compounds

The model assumes the potential for formation of a solid solution of Fe and Al as hydroxides. Litharge (PbO) and Ca₃(AsO₄)₂ were also assumed to form a solid solution with Fe and Al hydroxides [36].

Metal ion concentration was assumed to be affected by adsorption on hydrous ferric oxides (Hfo) [37,38] and silica gel [39]. Surface site densities and surface area used in this

study were 0.2 mol weak Hfo sites/mol Fe, 0.005 mol strong Hfo sites/mol Fe, and $600\,m^2\,g^{-1}$, respectively [40]. The surface complexation constants for Hfo were obtained from the Lawrence Livermore National Library (LLNL) database, sourced from a review by Dzombak and Morel [41]. A value of $600\,m^2\,g^{-1}$ was used to describe the silica gel surface area (Surf_s) for a 0.2 mol silanol (SiOH)/mol of Si system [32]. The ionisation constant for silica gel was taken from Iler [32] while the complexation constants for the silica gel surface with Pb^{2+} and Cd^{2+} were taken from Schindler et al. [42]. Values are shown in Table 5.

The metal concentration in the leachate is governed by the equilibrium states of solid compounds in the system. To account for the lack of information available regarding the kinetics of precipitation of most compounds, equilibrium was assumed for possible equilibrium-controlling species, including $Fe(OH)_3$, gibbsite, portlandite, calcite, and potential metal precipitates, such as litharge, alamosite, Pb_2SiO_4, cerussite, hydrocerussite, otavite, $CdSiO_3$, calcium arsenate, calcium chromate, eskolaite, and ferric arsenate. This function ensures the precipitation of compounds having saturation indices (SI's) close to the specified target SI, as shown in Table 7. SI is the ratio of the logarithm of the ion activity product to the logarithm of the solubility product. A positive SI indicates precipitation of the mineral while a negative SI indicates mineral solubilisation. Minerals possessing SI's between -2.0 and 2.0 are most likely to be the controlling mineral for constituent element solubility. In similar mineral series (e.g. oxides, hydroxides, carbonates), the mineral with the smallest positive SI will precipitate first due to its lowest interfacial free energy, according to the Ostwald Step Rule [43]. SI values for compounds relevant to each heavy metal waste were set at 0.0. An oversaturation SI of 0.75 was specified for calcite due to its tendency to supersaturate in liquors containing significant amount of silicate, as calcium preferentially adsorbs on silicate minerals [43].

4. Results and discussion

4.1. Leaching of Pb

Experimental and simulated Pb and Ca concentration profiles for Pb-contaminated cement leached with 0.1 M acetic acid are displayed in Fig. 2. The SI's of selected compounds at different leaching stages are provided in Table 8. In agreement with the portlandite dissolution rate, all the portlandite available on the cement surface dissolved within the first few minutes. This is consistent with Berner's findings for the degradation of concrete [24] and was found to be primarily responsible for the final solution pH. The modelling results (not shown here) indicated calcite dissolution occurred next and, when a pH of approximately 12 was attained, C–S–H dissolution played a role in further pH increase and metal ion release. Knowledge of the occurrence of each dissolution stage is important as it provides greater insight into factors controlling Pb release.

According to the model, the initial Pb presence observed in Fig. 2 was due to the release of free $Pb(OH)_2$ trapped within the cement pores. Decreasing this parameter within the model resulted in a significant decrease in initial Pb released. During the early stages of leaching, (30 s), all solid compounds possessed negative SI values (Table 8) with the dominant Pb species in solution being $PbAcetate_3^-$, $PbAcetate^+$, $PbAcetate_2$, and Pb^{2+}.

A pH increase after 3 min of leaching caused a rapid decrease in the Pb concentration (Fig. 2), suggested by the model as due to its precipitation as silicate species (alamosite and Pb_2SiO_4—Table 8). Simultaneously, the model indicates reformation of the C–S–H gel occurs, possibly contributing to the precipitation of these silicate species. As leaching progressed and the pH increased to 12 (Fig. 2), Pb released from

Table 7
Neutralisation or solubility constants of metal compounds specified in equilibrium

Compounds	Log neutralisation constant[a] (K_n) or solubility constant (K_{sp})
Alamosite ($PbSiO_3$)	$K_n = 5.67$[b]
$Ca_3(AsO_4)_2$	$K_{sp} = -18.9$[b]
$Ca_3(AsO_4)_2 \cdot 4H_2O$	$K_{sp} = -18.9$[c]
$Ca_3(AsO_4)_2 \cdot 6H_2O$	$K_{sp} = -18.9$[d]
Calcite ($CaCO_3$)	$K_n = 1.85$[b]
$Cd(OH)_2$	$K_n = 13.74$[b]
Cerussite ($PbCO_3$)	$K_n = -3.21$[b]
Eskolaite (Cr_2O_3)	$K_{sp} = -9.13$[b]
$Fe(OH)_3$	$K_n = 5.66$[b]
Gibbsite ($Al(OH)_3$)	$K_n = 7.76$[b]
Hydrocerussite ($Pb_3(CO_3)_2(OH)_2$)[c]	$K_n = 1.85$[b]
Litharge (PbO)	$K_n = 12.64$[b]
Otavite ($CdCO_3$)	$K_n = -1.77$[b]
Portlandite ($Ca(OH)_2$)	$K_n = 22.56$[b]

[a] Neutralisation constant (based on reaction of metal compound with H^+).
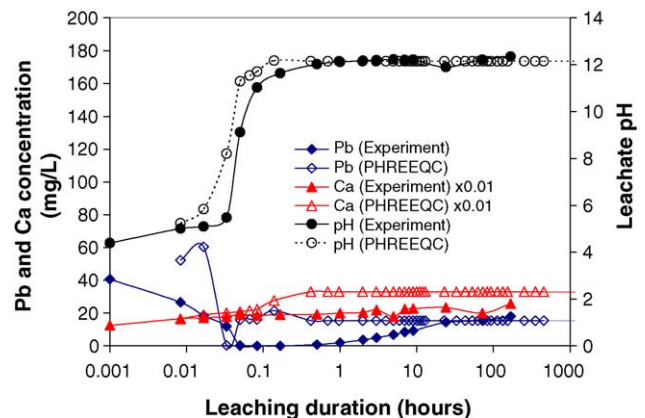[b] Taken from [51].
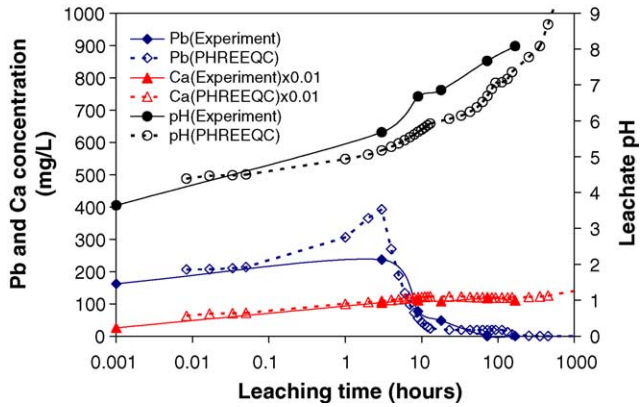[c] Taken from [52].
[d] Taken from [17].

Fig. 2. Experimental and modelling results for cementitious waste containing Pb tumbled with 0.1 M acetic acid. Ca concentrations are multiplied by 0.01.

Table 8
SI's of selected compounds at different stages of leaching for Pb-contaminated cement

	Formula	0.1 M acetic acid			0.6 M acetic acid		ML leachate		
		30 s	180 s	73 h	30 s	73 h	30 s	180 s	73 h
pH		5.2	11.3	12.2	4.4	6.7	8.7	8.9	10.9
pe		13.5	6.9	6.2	14.9	11.7	1.8	1.3	−4.2
Dominant Pb species in solution		$PbAcetate_3{}^-$ (60%)	$Pb(OH)_3{}^-$ (70%)	$Pb(OH)_3{}^-$ (95%)	$PbAcetate_3{}^-$ (88%)	$PbAcetate_3{}^-$ (94%)	PbOrganic X^+ (95%)	PbOrganic X^+ (95%)	PbOrganic X^+ (89%)
		$PbAcetate^+$ (25%)	$Pb(OH)_2$ (29%)	$Pb(OH)_2$ (5%)	$PbAcetate^+$ (6%)	$PbAcetate_2$ (4%)	PbOrganic X_2 (5%)	PbOrganic X_2 (5%)	$Pb(CO_3)_2{}^{2-}$ (7%)
		$PbAcetate_2$ (11%)	$PbOH^+$ (1%)		$PbAcetate_2$ (6%)	$PbAcetate^+$ (3%)			PbOrganic X_2 (4%)
		Pb^{2+} (4%)							
Alamosite	$PbSiO_3$	−4.4	1.9	1.7	−6.0	−0.75	−6.2	−4.2	0.77
Anglesite	$PbSO_4$	−3.0	−7.3	−8.0	−3.2	−2.5	−6.6	−5.9	−7.0
Brownmillerite	$Ca_4Al_2Fe_2O_{10}$	−81	−34	−25	−87	−68	−74	−71	−51
$Ca_2Al_2O_5{\cdot}8H_2O$	$Ca_2Al_2O_5{\cdot}8H_2O$	−27	−4.1	0.42	−32	−21	−28	−26	−19
$Ca_4Al_2O_7{\cdot}19H_2O$	$Ca_4Al_2O_7{\cdot}19H_2O$	−54	−6.7	1.4	−62	−42	−48	−45	−25
CaH_2SiO_4 (gel)	CaH_2SiO_4	−10	1.1	3.4	−11	−4.1	−8.7	−7.5	−2.0
Calcite	$CaCO_3$	−2.7	0.75	0.75	−3.5	0.75	0.75	0.75	0.75
Cerussite	$PbCO_3$	−1.1	−2.5	−5.1	−2.6	0.00	−0.92	0.00	−0.62
Ettringite	$Ca_6Al_2(SO_4)_3$ $(OH)_{12}.26H_2O$	−44	−6.9	5.1	−48	−26	−42	−40	−25
Hydrocerussite	$Pb_3(CO_3)_2(OH)_2$	−5.6	−0.89	−6.9	−11	−2.3	−4.6	−1.6	0.00
Hydrogarnet	$Ca_3Al_2(H_4O_4)_3$	−41	−5.2	1.1	−46	−31	−38	−35	−19
Lanarkite	$Pb(SO_4)O$	−5.4	−2.3	−3.7	−7.7	−3.9	−8.5	−6.6	−4.9
Litharge	PbO	−7.6	−0.19	−0.99	−9.7	−6.6	−7.1	−5.9	−3.1
Massicot	PbO	−7.8	−0.37	−1.2	−9.9	−6.8	−7.3	−6.1	−3.3
Pb_2SiO_4	Pb_2SiO_4	−12	2.0	0.95	−15	−7.1	−13	−9.8	−2.0

Fig. 3. Experimental and modelling results for cementitious waste containing Pb tumbled with 0.6 M acetic acid. Ca concentrations are multiplied by 0.01.

Fig. 4. Experimental and modelling results for cementitious waste containing Pb tumbled with ML leachate. Ca concentrations are multiplied by 0.1.

the cement increased again until it reached equilibrium. Here, according to the model, Pb exists predominantly in solution as hydroxy complexes ($Pb(OH)_3{}^-$ and $Pb(OH)_2$) and silicate precipitation remains the controlling mechanism for Pb stability. The quicker increase in Pb concentration above pH 12 for the modelling results (Fig. 2), despite similar pH profiles, may result from slower kinetics of Pb dissolution from precipitated $Pb(OH)_2$, due to its hydroxy complexes. This was not kinetically simulated in the model as it was considered a second order effect. Modelling also indicated the precipitation of Pb as a solid solution with Al and Fe hydroxides controlled its concentration. That is, removing litharge (PbO) from the solid solution led to a significant overestimation of Pb in the leachate.

Leaching with 0.6 M acetic acid (Fig. 3) saw the amount of Pb in the leachate increase during the first 3 h, after which, an increase in the pH produced a decrease in Pb concentration. The higher acetic acid concentration led to a slow increase in pH and a slow rate of Pb removal from the leachate. After 73 h of leaching, $PbAcetate_3{}^-$, $PbAcetate_2$, and $PbAcetate^+$ were the dominant Pb species in the solution with Pb-carbonate alluded to be governing Pb stability (Table 8).

Although modelling denoted Pb to be strongly adsorbed on hydrous iron oxide and silanol surfaces, as has been observed by other researchers [32,37,38], this effect was not found to dictate here due to the low amounts of soluble Fe and Si in the system, available as adsorption sites. This totalled less than 0.1 ppm of Pb adsorbed on hydrous iron oxide and silica gel surfaces for 0.1 M acetic acid and 6.8 ppm of Pb as Hfo_sOPb^+, 0.8 ppm of Pb as Hfo_sOPb^+, and less than 0.1 ppm of Pb adsorbed on the silica gel for 0.6 M acetic acid. Overall, precipitation was found to be the mechanism controlling Pb concentration in the leachate.

Pb, Ca and pH profiles as a function of leaching duration in the presence of ML leachate are provided in Fig. 4, with the SI's of various compounds at different stages of leaching by the ML leachate presented in Table 8. The initial increase in Pb (Fig. 4) is due to complexation of Pb with Organic X. This is illustrated in the model (Table 8), which shows com-
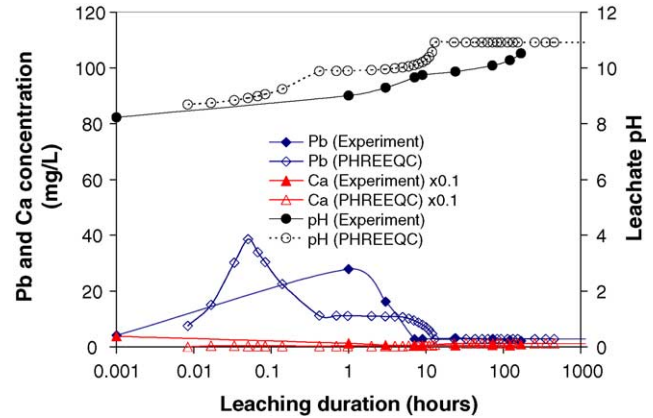
plexation of Pb with Organic X dominates Pb speciation in the solution below pH 10. Decreasing the stability constants of the Pb complexes led to an underestimation of Pb concentration, whereas increasing the stability constants resulted in overestimation of the dissolved Pb. At 180 s of leaching, the pH of the leachate had increased to 8.9, with Pb indicated to be precipitating as cerrusite. A further increase in pH to above 11 saw hydrocerussite and lead silicate precipitates likely to be the solubility controlling species.

It is also apparent from the model that C–S–H dissolution kinetics is governed by OH^- concentration. Omission of this species from the ML leachate simulation gives a constant pH following complete dissolution of portlandite and calcite. This is not observed in Fig. 4. The effect was also evident for the 0.1 and 0.6 M acetic acid leachates, but is more pronounced for the ML leachate due to its approximately neutral initial pH. That is, at an initial neutral pH and considering only H^+ in the kinetics of CSH dissolution, no significant driving force will be available to release the cement components. H^+ species lead to significant leaching only at low pH.

4.2. Leaching of Cd

Cd and Ca concentration profiles for the leaching of Cd-spiked cementitious waste by 0.1 and 0.6 M acetic acid are shown in Figs. 5 and 6, respectively. Model outputs for these systems are given in Table 10. The 0.1 M acetic acid initially released a high amount of Cd with the dominant species in solution indicated to be $CdAcetate^+$, $CdAcetate_2$, Cd^{2+}, and $CdAcetate_3{}^-$. Carbonate acted as the solubility controlling phase. The model specified the increase in pH to 12 (at 73 h of leaching) resulted in solubilisation of the carbonate and subsequent precipitation of Cd as its hydroxide and silicate.

The model was unable to simulate Cd release, between 3 and 80 h for the acetic acid, underestimating experimental results during this period (Fig. 6). This may be due to some factor in the Cd leaching/speciation, unaccounted for by the model in its current form, leading to the observed undershoot.
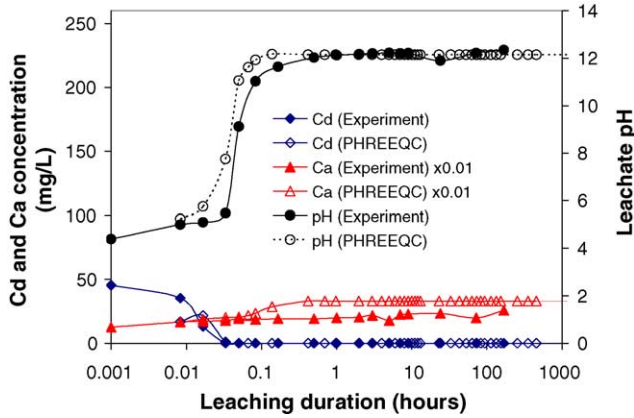
Fig. 5. Experimental and modelling results for cementitious waste containing Cd tumbled with 0.1 M acetic acid. Ca concentrations are multiplied by 0.01.

Both precipitation of Cd(OH)$_2$ in a solid solution with Al and Fe hydroxides and adsorption of Cd onto either the hydrous iron oxide or silica gel surfaces were reported by the model to be insignificant for controlling Cd concentration in the leachate. Less than 0.1 ppm of Cd was adsorbed on hydrous iron oxide and silica gel using 0.1 M acetic acid and 0.1 ppm of Cd was adsorbed as Hfo_sOCd$^+$ using 0.6 M acetic acid (after 73 h of leaching).

The modelling and experimental results for the leaching of Cd and Ca from cementitious waste by ML leachate are shown in Fig. 7. SI values are provided in Table 9. The model findings imply complexation of Cd with organic ligands increased the soluble Cd early in the leaching process. The increase in pH with time gives rise to the precipitation of Cd as carbonate and silicate species. Cd concentration was not experimentally monitored between 0 and 1 h, such that existence of the peak described by PHREEQC over this time frame cannot be confirmed here.
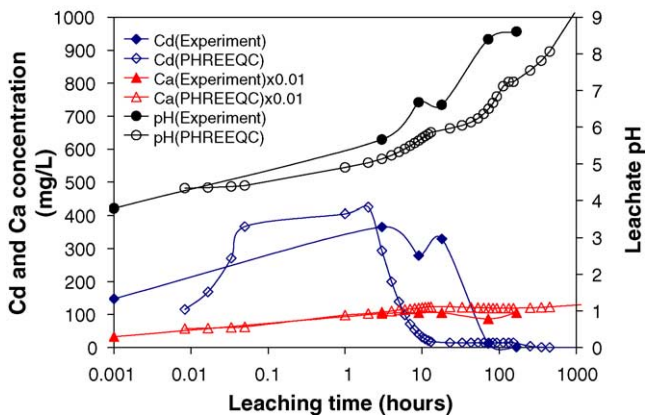

Fig. 7. Experimental and modelling results for cementitious waste containing Cd tumbled with ML leachate. Ca concentrations are multiplied by 0.01.

4.3. Leaching of As

Figs. 8 and 9 show the leaching profiles of As and Ca from cementitious waste using 0.1 and 0.6 M acetic acid, respec-

Fig. 8. Comparison between experimental and modelling results for cementitious wastes containing As tumbled with 0.1 M acetic acid. Ca concentration is multiplied by 0.01.

Fig. 6. Experimental and modelling results for cementitious waste containing Cd tumbled with 0.6 M acetic acid. Ca concentrations are multiplied by 0.01.
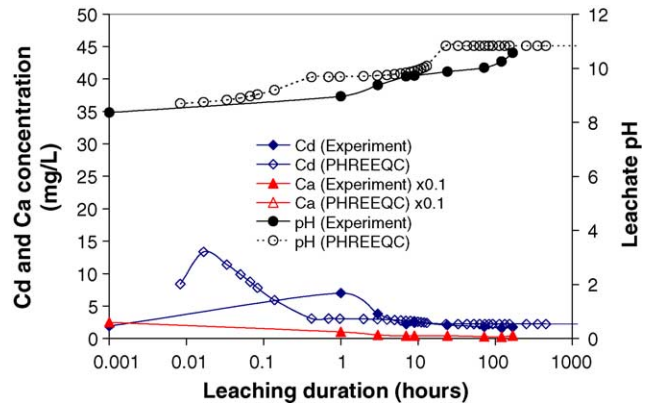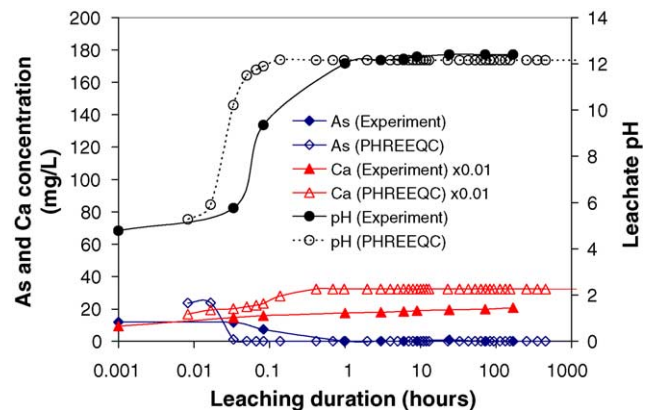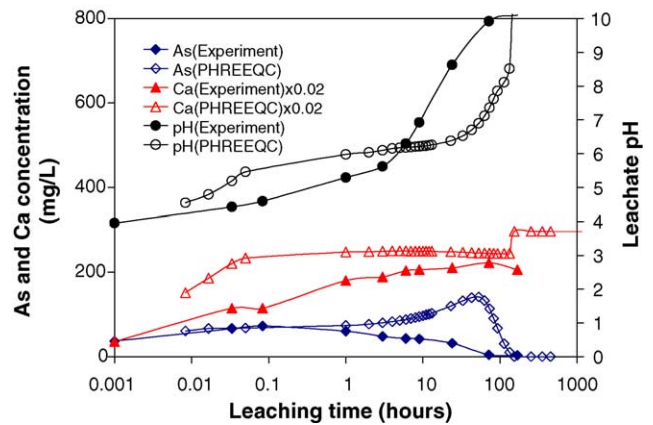

Fig. 9. Comparison between experimental and modelling results for cementitious wastes containing As tumbled with 0.6 M acetic acid. Ca concentration is multiplied by 0.02.

Table 9
SI's of selected compounds at different stages of leaching for Cd-contaminated cement

	Formula	0.1 M acetic acid			0.6 M acetic acid		ML leachate		
		30 s	180 s	73 h	30 s	73 h	30 s	180 s	73 h
pH		5.2	11.1	12.2	4.4	6.5	8.7	8.9	10.8
pe		13.5	0.7	−1.1	15.0	11.9	2.3	2.0	−2.7
Dominant Cd species in solution		$CdAcetate^+$ (45%)	$Cd(OH)_2$ (70%)	$Cd(OH)_2$ (80%)	$CdAcetate_2$ (47%)	$CdAcetate_2$ (48%)	CdOrganic X^+ (96%)	CdOrganic X^+ (96%)	CdOrganic X^+ (95%)
		$CdAcetate_2$ (32%)	$CdOH^+$ (15%)	$Cd(OH)_3{}^-$ (19%)	$CdAcetate^+$ (31%)	$CdAcetate_3{}^-$ (25%)	CdOrganic X_2 (3%)	CdOrganic X_2 (3%)	CdOrganic X_2 (3%)
		Cd^{2+} (19%)	$CdAcetate^+$ (8%)	$CdOH^+$ (1%)	$CdAcetate^{3-}$ (15%)	$CdAcetate^+$ (22%)	CdOrganic $X_3{}^-$ (1%)	CdOrganic $X_3{}^-$ (1%)	CdOrganic $X_3{}^-$ (1%)
		$CdAcetate_3{}^-$ (4%)	$CdAcetate_2$ (7%)	$Cd(OH)_4{}^{2-}$ (1%)	Cd^{2+} (7%)	Cd^{2+} (4%)			$Cd(CO_3)_2{}^{2-}$ (1%)
						$CdAcetate_4{}^{2-}$ (1%)			
Brownmillerite	$Ca_4Al_2Fe_2O_{10}$	−81	−34	−25	−88	−69	−66	−65	−52
$Ca_2Al_2O_5{\cdot}8H_2O$	$Ca_2Al_2O_5{\cdot}8H_2O$	−27	−4.1	0.52	−32	−22	−20	−20	−13
$Ca_4Al_2O_7{\cdot}19H_2O$	$Ca_4Al_2O_7{\cdot}19H_2O$	−54	−7.7	1.5	−62	−43	−40	−39	−26
CaH_2SiO_4 (gel)	CaH_2SiO_4	−10	0.52	3.4	−11	−4.4	−8.8	−7.7	−2.2
Calcite	$CaCO_3$	−2.8	0.75	0.75	−3.5	0.75	0.75	0.75	0.75
$Cd(OH)_2$	$Cd(OH)_2$	−8.2	0.00	0.00	−9.8	−6.7	−6.1	−5.6	−2.4
$CdSiO_3$	$CdSiO_3$	−6.0	1.3	1.9	−6.7	−1.5	−6.1	−4.7	0.74
$CdSO_4$	$CdSO_4$	−11	−14	−14	−9.8	−8.8	−12	−12	−13
Ettringite	$Ca_6Al_2(SO_4)_3$ $(OH)_{12}{\cdot}26H_2O$	−45	−8.4	5.2	−49	−27	−34	−34	−26
Hydrogarnet	$Ca_3Al_2(H_4O_4)_3$	−41	−5.7	1.2	−47	−32	−30	−29	−19
Otavite	$CdCO_3$	−2.2	−2.2	−4.5	−2.9	0.00	−0.25	0.00	0.00

Table 10
SI's of selected compounds at different stages of leaching for As-contaminated cement

	Formula	0.1 M acetic acid			0.6 M acetic acid		ML leachate		
		30 s	180 s	73 h	30 s	73 h	30 s	180 s	73 h
pH		5.3	11.5	12.2	4.5	7.3	7.9	8.4	11.5
pe		13.5	7.1	6.5	14.7	11.5	2.9	1.5	−5.6
Dominant As species in solution		$H_2AsO_4^-$ (94%) $HAsO_4^{2-}$ (6%)	AsO_4^{3-} (76%) $HAsO_4^{2-}$ (24%)	AsO_4^{3-} (96%) $HAsO_4^{2-}$ (4%)	$H_2AsO_4^-$ (81%) $HAsO_4^{2-}$ (19%)	$HAsO_4^{2-}$ (91%) $H_2AsO_4^-$ (9%)	$HAsO_4^{2-}$ (97%) $H_2AsO_4^-$ (3%)	$HAsO_4^{2-}$ (99%) $H_2AsO_4^-$ (1%)	AsO_4^{3-} (82%) $HAsO_4^{2-}$ (18%)
Arsenolite	As_2O_3	−48	−76	−81	−48	−53	−25	−23	−19
As_2O_5	As_2O_5	−20	−48	−53	−18	−25	−29	−31	−43
Brownmillerite	$Ca_4Al_2Fe_2O_{10}$	−80	−32	−25	−86	−63	−69	−67	−47
$Ca_2Al_2O_5 \cdot 8H_2O$	$Ca_2Al_2O_5 \cdot 8H_2O$	−27	−3.2	0.45	−31	−19	−22	−21	−11
$Ca_3(AsO_4)_2$	$Ca_3(AsO_4)_2$	−9.7	−0.27	−1.1	−11	−1.4	−10	−10	−7.2
$Ca_3(AsO_4)_2 \cdot 4H_2O$	$Ca_3(AsO_4)_2 \cdot 4H_2O$	−9.8	−0.31	−1.1	−11	−1.5	−10	−10	−7.2
$Ca_3(AsO_4)_2 \cdot 6H_2O$	$Ca_3(AsO_4)_2 \cdot 6H_2O$	−9.8	−0.28	−1.1	−11	−1.5	−10	−10	−7.2
$Ca_4Al_2O_7 \cdot 19H_2O$	$Ca_4Al_2O_7 \cdot 19H_2O$	−54	−5.1	1.4	−60	−37	−43	−41	−21
CaH_2SiO_4 (gel)	CaH_2SiO_4	−10	1.4	3.4	−11	3.4	−10	−8.7	−1.6
Calcite	$CaCO_3$	−2.9	0.75	0.75	−2.9	0.75	0.75	0.75	0.75
$FeAsO_4 \cdot 2H_2O$	$FeAsO_4$	−1.9	−16	−18	−0.36	−4.3	−6.3	−7.1	−13
Hydrogarnet	$Ca_3Al_2(H_4O_4)_3$	−41	−3.9	1.1	−45	−27	−32	−31	−15

tively. Initial SI's of selected minerals and SI's after 73 h of leaching are shown in Table 10. Fig. 8 shows an initial slow pH increase was experienced in the presence of 0.1 M acetic acid followed by a sharp increase after approximately three minutes. This pH increase was simulated by dissolution of the available portlandite, which is consumed very early in the leaching process. With increasing time and pH, portlandite dissolution was followed by calcite and C–S–H matrix dissolution. The latter is responsible for both calcium and further contaminant release at the alkaline pH.

The PHREEQC simulation suggests As was initially released from both the C–S–H matrix and discrete $Ca_3(AsO_4)_2$, mainly as $H_2AsO_4^-$ and low levels of $HAsO_4^{2-}$. The negative SI values of the selected solid compounds shown in Table 10 illustrate these compounds were soluble under this condition. Table 10 also indicates at low pH the solubility of As may be controlled by the solubility of ferric arsenate, which has an SI close to 0. As the leaching progresses, the leachate pH increases due to alkalinity release from the cement. This increase provides an increase in the SI's of many of the calcium minerals to above 0.0, signifying precipitation of these compounds in the system. Furthermore, according to the model, the pH increase also results in the solubilisation of ferric arsenate precipitate and the formation of a $Ca_3(AsO_4)_2$ precipitate with the released calcium (SI close to 0). In addition, the arsenic concentration was influenced by the formation of a solid solution with Fe and Al hydroxides, but this effect was not as significant as the precipitation of As as calcium arsenate.

Similar observations were made with 0.6 M acetic acid. At the higher acid concentration, a slower increase in pH provided a slower decrease in As concentration as calcium arsenate precipitation is more favourable at high pH. Again,

the precipitation of As as $Ca_3(AsO_4)_2$ was evoked to control As solubility.

Although the simulation showed As was strongly adsorbed on hydrous iron oxide surfaces, as has been similarly reported by van der Hoek et al. [44], only a small portion of As (<0.1 and 3.3 ppm Arsenic as $Hfo\_wOHAsO_4^{3-}$ after 73 h of leaching with 0.1 and 0.6 M acetic acid, respectively) was removed from solution by this mechanism. This is a consequence of the low level of Fe released ($\sim$3 mg L^{-1} with 0.1 M acetic acid and $\sim$40 mg L^{-1} with 0.6 M acetic acid from experimental results) in these systems and indicates precipitation of arsenate compounds plays a greater role in controlling arsenic concentration.

The municipal landfill leachate As leaching profile is shown in Fig. 10 with the SI's of selected compounds presented in Table 7 and reveals in the initial stages As was predominantly leached as $HAsO_4^{2-}$ and $H_2AsO_4^-$. Follow-
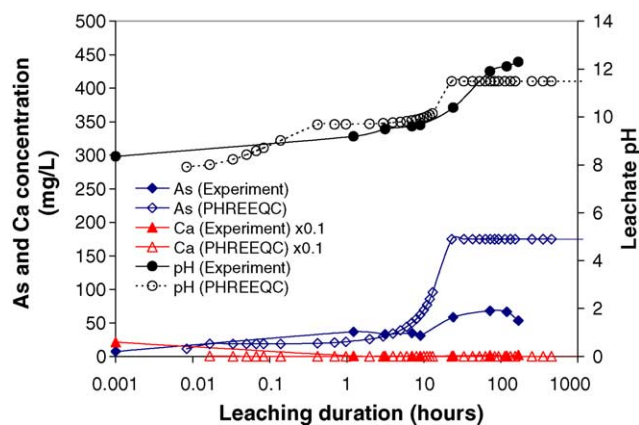

Fig. 10. Comparison between experimental and modelling results for cementitious wastes containing As tumbled with municipal landfill leachate.

ing 2 h of leaching, a dramatic increase in the simulated As solution level, due to an elevated C–S–H dissolution rate at the highly alkaline pH, contributed by the "OH⁻" component in Eq. (1). Removing the "OH⁻" term during C–S–H dissolution resulted in a constant leachate pH following portlandite and calcite consumption, which was not observed experimentally. After 73 h of leaching, as the pH increased to 11.5, the SI's of most compounds increased. However, it can be seen that the SI's of the calcium arsenate minerals remained well below 0.0 (−10), resulting in a higher modelled As concentration in solution than seen experimentally with the municipal landfill leachate. It is possible that in the pH 10–12 region As readsorbs onto components of the cement, such as ettringite, which the acetic acid-based leaches had previously dissolved [44]. This may be responsible for the lower experimentally observed As solution concentrations.

As a comparison, at a pH of 11.5 during leaching by the 0.1 M acetic acid (after 180 s of leaching—Table 10) the SI's of the calcium minerals are close to 0.0, indicating a lower solubility for As. It is clear from the simulation the high As concentration in the municipal landfill leachate is due to the preferential precipitation of calcium as calcium carbonate (SI = 0.75) resulting from the substantial level of dissolved inorganic carbon in the leachate. This supports previous inferences [13] regarding competition between calcium carbonate and calcium arsenate precipitation in municipal landfill leachate as controlling As concentration. Such a finding is important as it indicates leaching in municipal landfills may produce higher levels of arsenic than indicated by an acetic acid leachant, leading to inappropriate disposal of hazardous waste. Employing a leaching fluid containing carbonate alkalinity would improve the simulation of leaching in a municipal landfill leachate.

Minor variations in the pe of the ML leachate varied As speciation, although this did not necessarily affect As concentration. For instance, at an initial pe of −3.1 As mainly exists as As(V). A decrease to −3.5 resulted in 90% of the arsenic existing as As(III). As speciation analysis by ion chromatography/mass spectrometry showed the presence of only As(V) in the leachate sample after 7 days leaching by ML leachate, a pe of −3.1 was used for this simulation. It is important to note these experiments were conducted under ambient conditions without any attempt to establish a reducing environment. In a municipal landfill environment, As may exist as As(III) which is 60 times more toxic than As(V) [45], but can be more readily attenuated by precipitating as orpiment (As$_2$S$_3$) [46] and thioarsenite aqueous species [47].

Simulation of the As leaching from cement revealed increasing arsenic content in the C–S–H matrix and decreasing arsenic content in the free Ca$_3$(AsO$_4$)$_2$ produced an overestimation of the experimental As solution concentration. This suggests As is predominantly contained within the C–S–H matrix and not present as discrete Ca$_3$(AsO$_4$)$_2$, supporting previous electron microprobe findings [8]. However, at this time insufficient data is available to con-

firm metal containment mechanisms in C–S–H and similar phases.

The simulation indicated a substantial increase in As occurred after 2 h of leaching, however, this was not evident in the experimental work until after 10 h of leaching. The current rate constants were defined to give reasonable trends for all metal ions investigated (As and Cr) and for all leaching fluids. It is possible minor variations in the alkalinity of the cement-stabilised waste between batches and slightly different rate constants may occur within the different systems. Slight adjustments to the OH⁻ component of the C–S–H dissolution rate constant brought the model pH/time profile closer to experimental observations.

The model can act as a semi-predictive tool for the leaching of As from cementitious waste by providing speciation data at different leaching durations, which are difficult to obtain experimentally. The simulation shows leaching of As from cementitious waste is primarily governed by the dissolution rate of As from the C–S–H matrix and the concentration of As in the solution at high pH is influenced by the solubility of Ca$_3$(AsO$_4$)$_2$. The presence of carbonate alkalinity in the solution leading to the formation of CaCO$_3$ precipitate may therefore influence arsenate solubility. However, further studies are required to elucidate factors leading to the discrepancies between the experimental and modelling results particularly for the ML leachate in the long term.

4.4. Leaching of Cr

The Cr and Ca concentration profiles as a function of leaching duration using 0.1 and 0.6 M acetic acid are shown in Figs. 11 and 12, respectively. The SI's of selected compounds are shown in Table 11. Initially, when an acidic pH existed, Cr was mainly present as HCrO$_4^-$, Cr$_2$O$_7^{2-}$, and CrO$_4^{2-}$. The initial SI's of all Cr compounds in the presence of 0.1 or 0.6 M acetic acid are much lower than 0.0, illustrating the high solubility of Cr. As leaching progressed, the model identified CrO$_4^{2-}$ becoming the dominant species; however, the Cr remained highly soluble at all times.
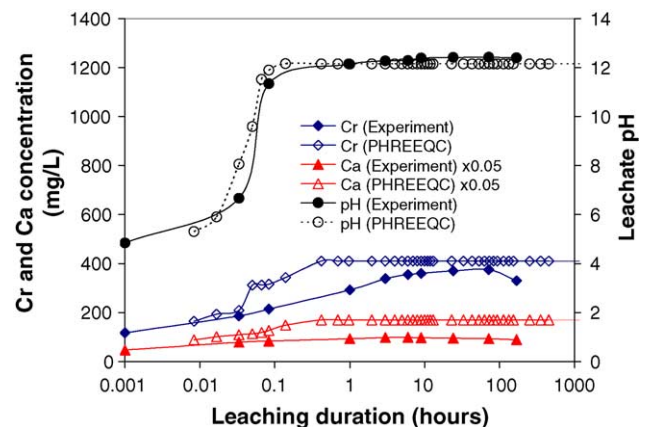

Fig. 11. Comparison between experimental and modelling results for cementitious wastes containing Cr tumbled with 0.1 M acetic acid.

Table 11
SI's of selected compounds at different stages of leaching for Cr-contaminated cement

	Formula	0.1 M acetic acid			0.6 M acetic acid		ML leachate		
		30 s	180 s	73 h	30 s	73 h	30 s	2 h	73 h
pH		5.3	9.6	12.1	4.5	7.5	9.3	10.0	12.1
pe		15.5	11.3	8.8	16.8	13.9	−5.2	5.3	2.0
Dominant Cr species in solution		$HCrO_4^-$ (79%) CrO_4^{2-} (11%) $Cr_2O_7^{2-}$ (10%)	CrO_4^{2-} (100%)	CrO_4^{2-} (100%)	$HCrO_4^-$ (73%) $Cr_2O_7^{2-}$ (24%) CrO_4^{2-} (2%)	CrO_4^{2-} (97%) $HCrO_4^-$ (3%)	$Cr(OH)_4^-$ (50%) $Cr(OH)_3$ (44%) $Cr(OH)_2^+$ (6%)	CrO_4^{2-} (100%)	CrO_4^{3-} (75%) CrO_4^{2-} (25%)
Brownmillerite,	$Ca_4Al_2Fe_2O_{10}$	−80	−46	−25	−86	−62	−63	−58	−41
$Ca_2Al_2O_5 \cdot 8H_2O$	$Ca_2Al_2O_5 \cdot 8H_2O$	−27	−10	0.40	−31	−19	−19	−16	−7.8
$Ca_4Al_2O_7 \cdot 19H_2O$	$Ca_4Al_2O_7 \cdot 19H_2O$	−54	−20	1.4	−60	−36	−37	−32	−15
CaH_2SiO_4 (gel)	CaH_2SiO_4	−10	−1.6	3.4	−11	−3.3	−7.6	−4.0	−0.78
Calcite	$CaCO_3$	−3.0	0.75	0.75	−3.8	0.75	0.75	0.75	0.75
Calcium chromate	$CaCrO_4$	−3.6	−2.3	−2.2	−3.8	−1.9	−45	−6.7	−6.9
Chromite	$FeCr_2O_4$	−26	−41	−51	−27	−35	0.00	−4.5	−5.2
Eskolaite	Cr_2O_3	−16	−31	−41	−17	−25	−6.7	0.00	−1.8
Hydrogarnet	$Ca_3Al_2(H_4O_4)_3$	−41	−15	1.1	−45	−27	−27	−24	−11

The simulation indicated Cr leaching derives from dissolution of the C–S–H matrix, releasing Cr trapped within the cement pores, and dissolution of free CrO_4^{2-} present on the C–S–H surface. Decreasing the proportion of free CrO_4^{2-} in the simulation resulted in an underestimation of Cr concentration illustrating Cr is mostly present as free CrO_4^{2-} supporting findings detailed in a previous publication [8].

Although Cr is known to adsorb on Al and Fe hydroxide surfaces below pH 8 [19], this model predicted the amount of Cr adsorbed to be insignificant (<0.1 ppm Cr as Hfo_sCrO_4^- using both 0.1 and 0.6 M acetic acid) due to the low level of Fe in the system. Formation of a solid solution of $CaCrO_4$ with Fe and Al hydroxides was also found to be insignificant.

The Cr leaching profile as a function of leaching duration by the municipal landfill leachate is shown in Fig. 13 with the SI's of selected compounds provided in Table 11. During the initial leaching period, the model indicated Cr(III) dominates the Cr species in the solution as $Cr(OH)_3$, $Cr(OH)_4^-$,

and $Cr(OH)_2^+$. The initial solubility of Cr was controlled by the solubility of chromite ($FeCr_2O_4$). As leaching progressed, leachate pH and redox potential increased resulting in the oxidation of Cr(III) to Cr(VI). This is illustrated by the domination of Cr as CrO_4^{2-} after 2 h of leaching (Table 11), while most Cr(III) appears to precipitate as its oxide/hydroxide. This is observed by the plateau in the Cr concentration between 1 and 10 h leaching. A further increase in pH saw dissolution of the Cr(III) precipitate and domination of CrO_4^{2-} in the solution, as indicated by the second plateau in Fig. 13.

The modelling provided evidence of Cr reduction during the early stages of leaching and was influenced by the pH and pe of the leachate. Variation in the reduction potential may result in variation of the Cr speciation. For example, a decrease of the reduction potential from −3.1 to −3.2 showed all the Cr present as Cr(III) and precipitated as its oxide/hydroxide. In the experimental study, after 2 h tumbling with the municipal landfill leachate, 25% of the Cr in the
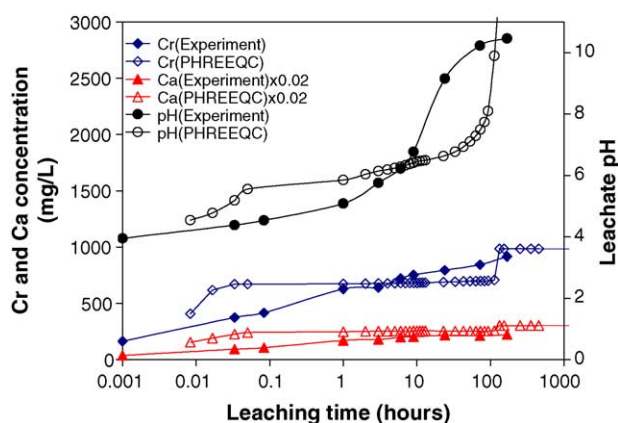

Fig. 12. Comparison between experimental and modelling results for cementitious wastes containing Cr tumbled with 0.6 M acetic acid.
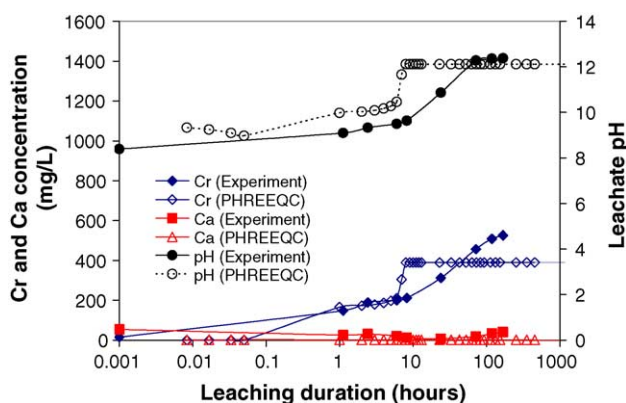

Fig. 13. Comparison between experimental and modelling results for cementitious wastes containing Cr tumbled with municipal landfill leachate.

solution was in the form of Cr(III) [13]. In the model simulation, although after 2 h of leaching the soluble Cr was mostly in the form of Cr(VI), some existed as a Cr(III) oxide precipitate (eskolaite). This suggests the precipitation of Cr(III) could be kinetically slow, resulting in Cr(III) being predominantly soluble during the experiment while in the model all the dissolved Cr(III) precipitated. It is important to note that, although the modelling study showed when leaching with this particular municipal landfill leachate the Cr existed as chromate ions, under actual mature landfill conditions (where leachate pH is typically between 6 and 8.5 and redox potential can be lower due to the absence of oxygen) Cr is more likely to exist as Cr(III), possessing a lower toxicity than Cr(VI) [48].

5. Conclusion

Due to the wide variations in waste and leachate characteristics, it is extremely difficult to develop a universal model capable of accurately predicting metal leaching from all available scenarios. The differences in these characteristics strongly influence the chemistry and dissolution rates of metals. However, if the compositions and dissolution rates of important waste constituents can be identified, metal leaching and speciation in the leachate can be predicted. This work has illustrated the capacity of PHREEQC for providing greater insight into the leaching of Pb, Cd, As, and Cr from cementitious waste in the presence of simple and complex leachants. In the presence of acetic acid, at low pH values, acetate complexes were predominant in solution whereas hydroxide species dominated at high pH values. In the presence of ML leachate, Organic X complexes dominated the heavy metal species in solution, while reduction of As(V) and Cr(V) dominated As and Cr speciation.

The model has indicated the same major phase dissolution rates are valid for Pb-, Cd-, As-, and Cr-contaminated wastes, illustrating its potential adaptability to cement containing different heavy metals. It also served to highlight the importance of hydroxide ions during dissolution of the C–S–H matrix and indicated carbonate and silicate species governed the solubility of Pb while carbonate, silicate and hydroxide species governed the solubility of Cd.

The model possesses the capacity for providing detailed information regarding the release of contaminants from waste with time under various conditions. Ultimately, information provided by the model may be valuable by assisting in decisions regarding choice of appropriate waste stabilisation techniques and conditions. However, in order to attain reliable results, information on both the composition of the waste and kinetics of the release has to be obtained. Defining waste composition can be a significant problem for unknown waste matrices. Moreover, information of kinetics of component release from the waste may not be easily found.

At present, the model has only been applied to short-term experimental data (7 days). The agreement between results suggests its use for predictions in the longer-term is possible. To confirm this, long-term leaching experiments and comparisons are required. Furthermore, greater attention is required to account for the effect of factors leading to the observed discrepancies between results that may have been overlooked in this version of the model.

References

[1] H.A. van der Sloot, L. Heasman, P. Quevauviller, Harmonization of Leaching/Extraction Tests, Elsevier, Amsterdam, 1997.
[2] P.L. Bishop, Leaching of inorganic hazardous constituents from stabilized/solidified hazardous wastes, Hazard. Waste Hazard. Mater. 5 (1988) 129–143.
[3] K.Y. Cheng, Controlling mechanisms of metals release from cement-based waste form in acetic acid solution, Ph.D. Thesis, University of Cincinnati, Cincinnati, 1991.
[4] S.R. Hillier, C.M. Sangha, B.A. Plunkett, P.J. Walden, Long-term leaching of toxic trace metals from Portland Cement Concrete, Cement Concrete Res. 29 (1999) 515–521.
[5] J. Macsik, A. Jacobsson, Leachability of V and Cr from LD-Slag/Portland Cement stabilised sulfide soil, Waste Manage. 16 (1996) 699–709.
[6] S. Trussell, B. Batchelor, Leaching of heavy metals from solidified wastes, Waste Manage. 13 (1993) 515–516.
[7] H.A. van der Sloot, D. Hoede, Long Term Leaching Behaviour of Cement Mortars, Petten Energieonderzoek Centrum, Netherland, 1997.
[8] P.G. Baker, P.L. Bishop, Prediction of metal leaching rates from solidified/stabilized wastes using the shrinking unreacted core leaching procedure, J. Hazard. Mater. 52 (1997) 311–333.
[9] B. Batchelor, Leach models: theory and applications, J. Hazard. Mater. 24 (1990).
[10] K.Y. Cheng, P.L. Bishop, Developing a kinetic leaching model for solidified/stabilized hazardous wastes, J. Hazard. Mater. 24 (1990) 213–224.
[11] M. Hinsenveld, A shrinking core model as a fundamental representation of leaching mechanisms in cement stabilized waste, Ph.D. Thesis, University of Cincinnati, Cincinnati, 1992.
[12] J.-C. Pierrard, J. Rimbault, M. Aplincourt, Experimental study and modelling of lead solubility as a function of pH in mixtures of ground waters and cement waters, Water Res. 36 (2002) 879–890.
[13] C.E. Halim, J.A. Scott, H. Natawardaya, R. Amal, D. Beydoun, G. Low, A comparison between acetic acid and landfill leachates for the leaching of Pb(II), Cd(II), As(V), and Cr(VI) from cementitious wastes, Environ. Sci. Technol. 38 (2004) 3977–3983.
[14] Standards Australia, Wastes, sediments and contaminated Soils. Part 3: preparation of leachates—bottle leaching procedure, Sydney, 1997.

[15] M. Atkins, F.P. Glasser, A. Kindness, Phase relations and solubility modeling in the CaO–SiO$_2$–Al$_2$O$_3$–MgO–SO$_3$–H$_2$O system, Mater. Res. Soc. Symp. 242 (1991) 387.

[16] U.R. Berner, Modelling the incongruent dissolution of hydrated cement minerals, Radiochim. Acta 44–45 (1988) 387–393.

[17] J.D. Allison, D.S. Brown, K.J. Novo-Gradac, MINTEQA2/PRODEFA2-A Geochemical Assessment Model for Environmental Systems version 3.0, Environmental Research Laboratory, Office of Research and Development, US Environmental Protection Agency, Athens, Georgia, 1990.

[18] U.R. Berner, Radionuclide Speciation in the Porewater of Hydrated Cement II. The Incongruent Dissolution of Hydrated Calciumsilicates, EIR, Wurenlingen, 1987.

[19] J.S. Geelhoed, J.C.L. Meeussen, S. Hillier, D.G. Lumsdon, R.P. Thomas, J.G. Farmer, E. Paterson, Identification and geochemical modeling of processes controlling leaching of Cr(VI) and other major elements from chromite ore processing residue, Geochim. Cosmochim. Acta 66 (2002) 3927–3942.

[20] C.E. Halim, R. Amal, D. Beydoun, J. Scott, G. Low, Implications of the structure of cementitious wastes containing Pb(II), Cd(II), As(V), and Cr(VI) on the leaching of metals, Cement Concrete Res. 34 (1998) 1093–1102.

[21] M.Y.A. Mollah, F. Lu, D.L. Cocke, An X-ray diffraction (XRD) and Fourier transform infrared spectroscopic (FT-IR) characterization of the speciation of arsenic (V) in Portland Cement Type-V, Sci. Total Environ. 224 (1998) 57–68.

[22] C. Oman, Comparison between the predicted fate of organic compounds in landfills and the actual emissions, Environ. Sci. Technol. 35 (2001) 232–239.

[23] D.S. Brown, R.E. Carlton, L.A. Mulkey, Development of Land Disposal Decisions for Metals Using MINTEQ Sensitivity Analysis, Environmental Research Laboratory, Office of Research and Development, US EPA, Athens, 1986.

[24] U.R. Berner, Modelling porewater chemistry in hydrated Portland Cement, Mater. Res. Symp. (1987).

[25] L. Chou, R.M. Garrels, R. Wollast, Comparative study of the kinetics and mechanisms of dissolution of carbonate minerals, Chem. Geol. 78 (1989) 269–282.

[26] K.O. Kjellsen, H. Justnes, Revisiting the microstructure of hydrated tricalcium silicate—a comparison to Portland Cement, Cement Concrete Res. 26 (2004) 947–956.

[27] V.V. Hardikar, E. Matijevic, Influence of ionic and nonionic dextrans on the formation of calcium hydroxide and calcium carbonate particles, Colloids Surf. A 186 (2001) 23–31.

[28] J. Yu, M. Lei, B. Cheng, X. Zhao, Effects of PAA additive and temperature on morphology of calcium carbonate particles, J. Solid State Chem. 177 (2004) 681–689.

[29] P. Joye, P. Demont, Density of calcium hydroxide and the role of that material in the shrinkage of Portland Cement, J. Chim. Phys. Phys.-Chim. Biol. 26 (1929) 317–318.

[30] D.B. Leineweber, Production of calcium magnesium acetate (CMA) from dilute aqueous solutions of acetic acid, M.Sc. Thesis, University of Wisconsin-Madison, Madison, 2002.

[31] R.L. Segall, R.S.C. Smart, P.S. Turner, Oxide surfaces in solution, in: J. Nowotny, L.C. Dufour (Eds.), Surface and Near-Surface Chemistry of Oxide Materials, Elsevier, Amsterdam, 1988.

[32] R.K. Iler, The Chemistry of Silica, John Wiley & Sons, New York, 1979.

[33] W.H. Casey, C. Ludwig, Silicate mineral dissolution as a ligand-exchange reaction, in: A.F. White, S.L. Brantley (Eds.), Chemical Weathering Rates of Silicate Minerals, Mineralogical Society of America, Bookcrafters, Inc., Michigan, 1995, Chapter 3, pp. 87–117.

[34] F.L.L. Muller, Interactions of copper, lead and cadmium with the dissolved, colloidal and particulate components of estuarine and coastal waters, Marine Chemistry 52 (1996) 245–268.

[35] P. Lubal, D. Siroky, D. Fetsch, J. Havel, The acidobasic and complexation properties of humic acids—study of complexation of Czech humic acids with metal ions, Talanta 47 (1998) 401–412.

[36] J.L. Jambor, Nomenclature of the alunite supergroup: reply, Can. Mineral. 38 (2000) 1298–1303.

[37] D. Kovacevic, A. Pohlmeier, G. Ozbas, H.-D. Narres, M.J.N. Kallay, The adsorption of lead species on goethite, Colloids Surf. A 166 (2000) 225–233.

[38] J.E. van Benschoten, W.H. Young, M.R. Matsumoto, B.E. Reed, A nonelectrostatic surface complexation model for lead sorption on soils and mineral surfaces, J. Environ. Qual. 27 (1998) 24–30.

[39] D.L. Dugger, J.H. Stanton, B.N. Irby, B.L. McConnell, W.W. Cummings, R.W. Maatman, The exchange of twenty metal ions with the weakly acidic silanol group of silica gel, J. Phys. Chem. 68 (1964) 757–760.

[40] J.M. Zachara, D.C. Girvin, R.L. Schmidt, C.T. Resch, Chromate adsorption on amorphous iron oxyhydroxide in the presence of major groundwater ions, Environ. Sci. Technol. 21 (1987) 589–594.

[41] D.A. Dzombak, F.M.M. Morel, Surface Complexation Modeling-Hydrous Ferric Oxide, John Wiley, New York, 1990.

[42] P.W. Schindler, B. Furst, R. Dick, P.U. Wolf, Ligand properties of surface silanol groups, J. Colloid Interface Sci. 55 (1976) 469–475.

[43] W. Stumm, J.J. Morgan, Aquatic Chemistry—Chemical Equilibria and Rates in Natural Waters, John Wiley & Sons Inc., New York, 1996.

[44] E.E. van der Hoek, P.A. Bonouvrie, R.N.J. Comans, Sorption of As and Se on mineral components of fly ash: relevance for leaching processes, Appl. Geochem. 9 (1994) 403–412.

[45] J.I. Ryu, S. Gao, R.A. Dahlgren, R.A. Zierenberg, Arsenic distribution, speciation and solubility in shallow groundwater of Owens Dry Lake, California, Geochim. Cosmochim. Acta 66 (2002) 2981–2994.

[46] P. O'Neill, Arsenic, in: B.J. Alloway (Ed.), Heavy Metals in Soils, Blackie and Son Ltd., Glasgow, 1990, pp. 83–99.

[47] R.T. Wilkin, D. Wallschlaeger, R.G. Ford, Speciation of arsenic in sulfidic waters, Geochem. Trans. 4 (2003) 1–7.

[48] M. Costa, Potential hazards of hexavalent chromate in our drinking water, Toxicol. Appl. Pharmacol. 188 (2003) 1–5.

[49] C.E. Halim, R. Amal, H. Natawardaya, D. Beydoun, J. Scott, G. Low, J. Cattle, Comparison of leaching of Pb(II), Cd(II), As(V), and Cr(VI) from cementitious wastes using acetic acid and landfill leachates, in: The Eighteenth International Conference on Solid Waste Technology and Management, Philadelphia, 2003.

[50] E.J. Reardon, An ion interaction model for the determination of chemical equilibria in cement/water systems, Cement Concrete Res. 20 (1990) 175–192.

[51] E3/6 Database, Lawrence Livermore National Laboratory Database 8, Release 6, California, 1998.

[52] A.H. Truesdell, B.F. Jones, A computer program for calculating chemical equilibria of natural water, J. Res. U.S. Geol. Survey 2 (1974) 233–274.